

Increased Cation Conductance in Human Erythrocytes Artificially Aged by Glycation

Yuliya V. Kucherenko · Shefalee K. Bhavsar ·
Valentin I. Grischenko · Uwe R. Fischer ·
Stephan M. Huber · Florian Lang

Received: 29 October 2009 / Accepted: 12 May 2010 / Published online: 6 June 2010
© Springer Science+Business Media, LLC 2010

Abstract Excessive glucose concentrations foster glycation and thus premature aging of erythrocytes. The present study explored whether glycation-induced erythrocyte aging is paralleled by features of suicidal erythrocyte death or eryptosis, which is characterized by cell membrane scrambling with subsequent phosphatidylserine exposure at the cell surface and cell shrinkage. Both are triggered by increases of cytosolic Ca^{2+} concentration ($[\text{Ca}^{2+}]_i$), which may result from activation of Ca^{2+} permeable cation channels. Glycation was accomplished by exposure to high glucose concentrations (40 and 100 mM), phosphatidylserine exposure estimated from annexin binding, cell shrinkage from decrease of forward scatter, and $[\text{Ca}^{2+}]_i$ from Fluo3-fluorescence in analysis via fluorescence-activated cell sorter. Cation channel activity was determined by means of whole-cell patch clamp. Glycation of total membrane proteins, immunoprecipitated TRPC3/6/7, and immunoprecipitated L-type Ca^{2+} channel proteins was estimated by Western blot testing with polyclonal antibodies used against

advanced glycation end products. A 30–48-h exposure of the cells to 40 or 100 mM glucose in Ringer solution (at 37°C) significantly increased glycation of membrane proteins, hemoglobin (HbA_{1c}), TRPC3/6/7, and L-type Ca^{2+} channel proteins, enhanced amiloride-sensitive, voltage-independent cation conductance, $[\text{Ca}^{2+}]_i$, and phosphatidylserine exposure, and led to significant cell shrinkage. Ca^{2+} removal and addition of Ca^{2+} chelator EGTA prevented the glycation-induced phosphatidylserine exposure and cell shrinkage after glycation. Glycation-induced erythrocyte aging leads to eryptosis, an effect requiring Ca^{2+} entry from extracellular space.

Keywords TRPC · Calcium channels · Glycation · Hemoglobin · $\alpha 1\text{C}$ peptide

Suicidal erythrocyte death or eryptosis and erythrocyte aging share several features with apoptosis of nucleated cells, such as cell membrane scrambling with breakdown of cell membrane phosphatidylserine asymmetry, cell membrane blebbing, and cell shrinkage, all typical features of apoptosis in nucleated cells (Lang et al. 2003b, 2008; Lew et al. 2007). Eryptosis could be triggered by increase of cytosolic Ca^{2+} concentration ($[\text{Ca}^{2+}]_i$) (Lang et al. 2003b). In untreated erythrocytes $[\text{Ca}^{2+}]_i$ is very low (in the range of 10–100 nM; Tiffert et al. 2003) but may be rapidly increased after Ca^{2+} entry through Ca^{2+} -permeable cation channels (Lang et al. 2008). The existence of two types of nonselective Ca^{2+} -permeable cation channels has been disclosed by the patch clamp technique, i.e., the voltage-gated channel coupled to an acetylcholine receptor (Baunbaek and Bennekou 2008) and a voltage-independent cation channel (Huber et al. 2001). The latter was shown to be stimulated by osmotic shock and oxidative stress (Lang

Y. V. Kucherenko · S. K. Bhavsar · F. Lang (✉)
Department of Physiology, Institute I,
Eberhard-Karls-Universität Tübingen, Gmelinstr. 5,
72076 Tübingen, Germany
e-mail: florian.lang@uni-tuebingen.de

Y. V. Kucherenko · V. I. Grischenko
Institute for Problems of Cryobiology and Cryomedicine,
Ukrainian National Academy of Sciences, Kharkov 61015,
Ukraine

U. R. Fischer
Center for Theoretical Physics, Department of Physics and
Astronomy, Seoul National University, Seoul 151-747, Korea

S. M. Huber
Department of Radiation Oncology, Eberhard-Karls-Universität
Tübingen, 72076 Tübingen, Germany

et al. 2008), events that accompany cell aging (Avogaro et al. 2010). Erythrocyte aging may further be due to impaired extrusion of Ca^{2+} resulting from a decline of the plasma membrane Ca^{2+} pump activity (Lew et al. 2007).

The aging of erythrocytes could be triggered by exposure to excessive concentrations of glucose, which reacts in an open aldehyde form nonenzymatically with the NH_2 -terminal amino of the β -chain of proteins, forming a stable covalent link (Bunn and Higgins 1981). Because glycation is usually a slow reaction (weeks and months), most in vitro experiments were carried out at high glucose concentrations (30–100 mM) (Arai et al. 1987; Bilgin and Tukul 1996; Bookchin et al. 2009; Booth et al. 1997; Gonzalez Flecha et al. 1999; Jain and Lim 2001). The results on erythrocytes demonstrated a dramatic decline in the activity of Na^+ , K^+ -ATPase, Ca^{2+} -ATPase, and Cu-Zn superoxide dismutase as well as a decrease of erythrocyte membrane fluidity as a result of glycation of hemoglobin and membrane proteins (Arai et al. 1987; Bilgin and Tukul 1996; Gonzalez Flecha et al. 1999). In nucleated cells, diabetes mellitus has been shown to enhance the transcript levels and protein expressions of NHE1 (Cukiernik et al. 2004; Wu et al. 2008). Additional glycation of normally N-glycated proteins could affect their folding and thus might impair substrate access to the transporters (Chen et al. 2006).

The glycation pattern was also found to regulate the activity of nonselective cation channels related to transient receptor potential (TRP) family of proteins (Dietrich et al. 2003). TRPC6 channels were shown to be expressed in erythroid progenitor cells (Chu et al. 2004). In human red blood cell ghost, antibodies against TRPC6 or TRPC3/6/7 were shown to inhibit Ca^{2+} entry (Foller et al. 2008). TRPC6 channels are heavily glycosylated, with two extracellular N-linked glycosylated sites, while TRPC3 is a monoglycosylated protein (Vannier et al. 1998). Elimination of the glycosylated site of TRPC6, which is lacking in TRPC3, transformed the receptor-regulated TRPC6 channels with low basal activity into a constitutively active double (inward and outward) rectifying TRPC3-like ion channel. Conversely, an additional glycosylation site in TRPC3 reduced its basal activity (Dietrich et al. 2003).

The products of nonenzymatic reaction between monosaccharides (especially between glucose) and proteins may play a significant role in the process of cell aging (Lew et al. 2007). In vitro prepared products of advanced glycation show toxic properties (Booth et al. 1997). Glycotoxins are immunogenic, and they facilitate the formation of cross-linked bonds in proteins (Vlassara et al. 1992). The appearance of cross-linked proteins was also observed during the process of cell aging and it is considered a secondary complication in diabetes (Booth et al. 1997).

The amount of glycosylated proteins, formed during the incubation of erythrocytes with high concentrations of glucose, depends on the age of the erythrocyte population (Lew et al. 2007). Age-dependent accumulation of glycosylated hemoglobin (HbA_{1c}) was similarly observed in fractions of density-separated cells—that is, less dense young erythrocytes are separated from the more dense old erythrocytes (Lew et al. 2007).

The aim of the present study was to define the effect of glucose-induced glycation on channel activity and Ca^{2+} entry. To this end, in vitro erythrocytes were exposed to 40 mM or 100 mM glucose for 2 days at 37°C .

Materials and Methods

Erythrocytes

Erythrocytes were drawn from healthy volunteers, who signed informed consent. The study has been approved by the ethical commission of the University of Tübingen (184/2003 V). Experiments were performed at room temperature (22 – 26°C) with banked erythrocyte concentrates provided by the blood bank of the University of Tübingen or with freshly drawn erythrocytes from a healthy donor (experiments on age-fractionated erythrocytes). Erythrocytes were washed twice ($1200 \times g$, 5 min, 22°C) in physiological saline (Ringer solution in mM: 145 NaCl, 5 KCl, 2 MgCl_2 , 1 CaCl_2 , 5 glucose, 10 HEPES/NaOH, pH 7.4).

In vitro glycation was accomplished by incubation of erythrocytes in Ringer solution containing 40 mM (or 100 mM) glucose for 2 days at 37°C . After the glycation procedure, the erythrocytes were washed three times in the same solution as above.

Determination of HbA_{1c}

HbA_{1c} was determined by calorimetry from the reaction of 5-oxymethylphurphur (the product of the acid hydrolysis of glucose, which was covalently bound to proteins) with thiobarbituric acid (Fluckiger and Winterhalter 1976). Measurements were made at 443 nm with a Pye Unicam SP8000 spectrophotometer (Pye Unicam, Cambridge, UK). Because the thiobarbituric acid test is not specific for phurphur, the thiobarbituric acid reaction with HbA, which was not treated with the organic acid, was taken as control.

Washed cells were then fractionated as described previously (Turker and Young 1982). To this end, erythrocytes at a hematocrit of 80% were centrifuged at $2500 \times g$ for 60 min. The top fraction (one-third) was transferred to another test tube and recentrifuged ($2500 \times g$, 60 min, 22°C). After that, the top fraction, which was enriched with young erythrocytes, was collected. The cells on the bottom

(one-third) of the first tube, which were enriched with old cells, were collected and used as a fraction of “old” cells. The rest of the cells were used as a fraction of “middle” cells. Hemoglobin was obtained after hypotonic hemolysis of the fractionated cells in 5 mM Na-phosphate buffer (1:20) and centrifugation at $12,000 \times g$ (15 min, 4°C). Before the measurements, cells were incubated in Na-phosphate-buffered physiological saline (pH 7.4) with or without 40 mM glucose for 30 h at 37°C.

Phosphatidylserine Exposure and Forward Scatter

Erythrocytes were washed once in Ringer solution containing 5 mM CaCl_2 . The cells were then stained with annexin V-Fluos (Roche, Mannheim, Germany) at a 1:500 dilution in 5 mM Ca^{2+} -containing Ringer solution. After 15 min, samples were washed once and resuspended in 5 mM Ca^{2+} -containing Ringer solution and then measured by flow cytometric analysis (FACSCalibur; Becton Dickinson, Heidelberg, Germany). Annexin V-fluorescence intensity was measured in fluorescence channel FL-1 with an excitation wavelength of 488 nm and an emission wavelength of 530 nm. The size (volume) of the cells was determined by forward scatter. During determination of the forward scatter, scattered light is collected by a detector. The parameter is referred to as *small angle light scatter*, *forward angle lights scatter*, or, most commonly, *forward scatter*. Forward scatter is proportional to cell size; the bigger the cell, the more light is scattered, and the larger the detected signal (Shapiro 2003).

Intracellular Ca^{2+}

Erythrocytes were washed in Ringer solution containing 5 mM CaCl_2 and then loaded with Fluo-3/AM (Calbiochem, Bad Soden, Germany) in Ringer solution containing 5 mM CaCl_2 and 2 μM Fluo-3/AM. The cells were incubated at 37°C for 20 min and washed once in Ringer solution containing 5 mM CaCl_2 . The Fluo-3/AM-loaded erythrocytes were resuspended in 200 μl Ringer solution. Then Ca^{2+} -dependent fluorescence intensity was measured in fluorescence channel FL-1 by fluorescence-activated cell sorter (FACS) analysis. Because the analysis does not provide a fluorescence ratio, Fluo3 does not allow the calculation of the cytosolic Ca^{2+} concentration.

Electrophysiology

Patch clamp recordings were performed at room temperature. The patch electrodes were made of borosilicate glass capillaries (150 TF-10, Clark Medical Instruments) using a horizontal DMZ puller (Zeitz). Pipettes with high resistance

from 12 to 17 M Ω were connected via an Ag-AgCl wire to the head stage of an EPC 9 patch clamp amplifier (Heka). Data acquisition and data analysis were controlled by a computer equipped with an ITC 16 interface (Instrutech) and Pulse software (Heka). For current measurements, erythrocytes were held at a holding potential (V_h) of -30 mV, and 200-ms pulses from -100 to $+100$ mV (or to $+80$ mV) were applied in increments of $+20$ mV. The original current traces are depicted without filtering (acquisition frequency of 3 kHz). The currents were analyzed by averaging the current values measured between 90 and 190 ms of each square pulse (current-voltage relationship). The applied voltages refer to the cytoplasmic face of the membrane with respect to the extracellular space. The offset potentials between both electrodes were zeroed before sealing. The liquid junction potentials between bath and pipette solutions, and between the bath solutions and the salt bridge (filled with NaCl bath solution) were calculated according to Barry and Lynch (1991). Data were corrected for liquid junction potentials.

Only the cells that had characteristic echinocytic shape after the glycation procedure were used for patch clamp experiments. Recordings were obtained after reaching a >10 G Ω seal.

For whole-cell recording, the pipette solutions consisted of (in mM): 125 Na-gluconate, 10 NaCl, 1 MgCl_2 , 1 MgATP, 1 EGTA, 10 HEPES/NaOH (pH 7.4) or 118 mM Cs-aspartate, 10 Na-aspartate, 0.7 CaCl_2 , 3 MgCl_2 , 12 EGTA, 10 HEPES (pH 7.4) or 118 mM Cs-aspartate, 10 Na-aspartate, 0.1 CaCl_2 , 3.16 MgCl_2 , 10 Cs-BAPTA, 10 HEPES (pH 7.4). On-cell patch clamp recordings were performed with KCl pipette solution (150 KCl, 10 HEPES, pH 7.4). The NaCl Ringer bath solution contained (in mM): 145 NaCl, 5 KCl, 2 MgCl_2 , 1 CaCl_2 , 5 (or 40, or 100) glucose, 10 HEPES/NaOH (pH 7.4). In the experiments, where Cl^- was substituted with gluconate, the solution contained (in mM): 150 Na-gluconate, 2 MgCl_2 , 1 CaCl_2 , 5 (or 40, or 100) glucose, 10 HEPES/NaOH (pH 7.4). The NMDG-Cl and CaCl_2 bath solutions contained (in mM): 160 NMDG (titrated with HCl to pH 7.4) or 100 CaCl_2 , 10 HEPES (titrated with NMDG or CaOH_2 to pH 7.4). Chemicals were obtained from Sigma (Taufkirchen, Germany) and were of the highest grade available.

Western Blot

Human erythrocytes were incubated in Ringer solution (control) or in Ringer solution containing 40 mM or 100 mM glucose for 48 h. After incubation, 200- μl erythrocyte pellets were lysed in 50 ml of 20 mM HEPES (N-2-hydroxyethylpiperazine-N-2-ethanesulfonic acid)/NaOH (pH 7.4). Ghost membranes were pelleted ($15,000 \times g$ for 20 min at 4°C) and additionally lysed in 200 μl lysis buffer (50 mM

Tris-HCl, pH 7.5, 150 mM NaCl, 1% Triton X-100, 0.5% SDS, 1 mM NaF, 1 mM Na₃VO₄, 0.4% β -mercaptoethanol) containing protease inhibitor cocktail (Sigma, Taufkirchen, Germany). The samples (50 μ g of protein each) were solubilized in Laemmli sample buffer at 95°C for 5 min and resolved by 10% sodium dodecyl sulfate–polyacrylamide gel electrophoresis. For immunoblotting, proteins were electrotransferred onto a PVDF (polyvinylidene difluoride) membrane and blocked with 5% nonfat milk in Tris-buffered saline–0.10% Tween 20 at room temperature for 1 h. After that, the membrane was incubated with affinity-purified rabbit polyclonal antibody TRPC3/6/7 (H-100) (sc-20111; Santa Cruz Biotech) or goat polyclonal antibody to AGE serum (Acris Biosciences), that detects advanced glycation end-product epitopes, or with goat polyclonal antibody L-type Ca²⁺ CP α 1C (A-20) (sc-16230; Santa Cruz Biotech) at 4°C overnight. Subsequently, blocked blots were washed and additionally incubated with secondary anti-rabbit or anti-goat antibodies (1:5000; Cell Signaling, Frankfurt, Germany), conjugated to horseradish peroxidase, for 1 h at 22°C. Antibody binding was detected after washing the blots with a Super Signal Chemiluminescence detection procedure (Cell Signaling, Frankfurt, Germany).

Immunoprecipitation and Subsequent Detection of Glycated TRPC Channels and L-type Ca²⁺-Channels

The proteins were immunoprecipitated with TRPC3/6/7 antibody with subsequent Western blot that used antibodies directed against glycated proteins. Briefly, 1500 μ g of total protein were immunoprecipitated with 6 μ g (2 μ g/500 μ g total protein) of TRPC3/6/7 (H-100) (sc-20111; Santa Cruz Biotech), using the Dynabeads Protein G immunoprecipitation kit from Invitrogen following the manufacturer's protocol. Then the subsequent Western blot with goat polyclonal antibody to AGE-serum (Acris Biosciences) was performed.

Statistics

Data are expressed as arithmetic means \pm standard error of the mean (SEM), and unpaired two-tailed *t*-test or analysis of variance (ANOVA) (Student–Newman–Keuls multiple comparisons test) was used as appropriate; *P* < 0.05 was considered statistically significant.

Results

Before treatment with glucose-rich extracellular fluid, the percentage of hemoglobin being glycated was less than 3% (1.89 \pm 0.61%, *n* = 3). The percentage depended on the age of the erythrocytes (Fig. 1). It was below 3% in young

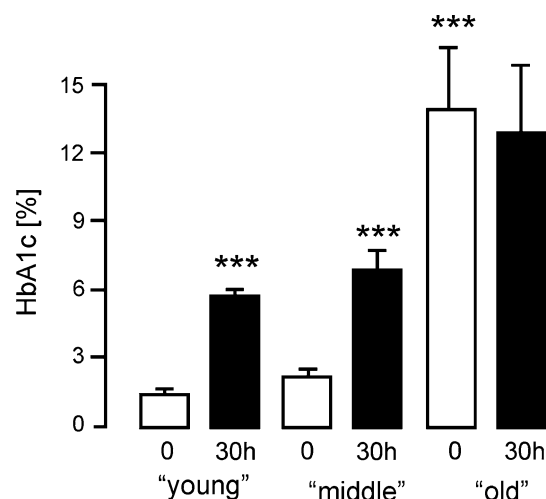


Fig. 1 Increase in glycated HbA concentration ([HbA_{1c}]) in age-fractionated cells after exposure to 40 mM glucose. Arithmetic means \pm SEM of the percentage of HbA_{1c} to the total HbA in age-fractionated erythrocytes after 30-h treatment with Ringer solution in the presence of 40 mM glucose (*n* = 3). *** Significant difference from control (open bars) and from young and middle erythrocytes (open bar), respectively, *P* < 0.001, ANOVA

and middle-aged erythrocytes but approached approximately 12% in old erythrocytes. Exposure of human erythrocytes for 30 h to 40 mM glucose was followed by a marked and statistically significant increase of HbA_{1c} in young and middle-aged erythrocytes (Fig. 1). After treatment, the percentage of HbA_{1c} in young and middle-aged erythrocytes was half that of old erythrocytes, indicating that the treatment indeed efficiently triggered protein glycation in young erythrocytes to values close to those of older erythrocytes.

In a next series of experiments, we explored whether the enhanced glycation was paralleled by stimulation of eryptosis, which is characterized by cell membrane scrambling and cell shrinkage (Lang et al. 2008). Annexin V binding was used to identify erythrocytes with scrambled cell membrane phospholipids, thus exposing phosphatidylserine at the cell surface. As illustrated in Fig. 2a, b, a 48-h glucose treatment led to a marked and statistically significant increase of the percentage of annexin V binding erythrocytes, which was significantly more pronounced after exposure to 100 mM glucose than after exposure to 40 mM glucose.

Because phospholipid scrambling could result from increase of cytosolic Ca²⁺ concentration ([Ca²⁺]_i) (Lang et al. 2003a), Fluo3 fluorescence was used to test whether exposure to high concentrations of glucose modified [Ca²⁺]_i. As illustrated in Fig. 2c, d the treatment with high glucose concentrations was indeed followed by a statistically significant increase in Fluo3 fluorescence.

Increase of cytosolic Ca²⁺ activity is further known to trigger cell shrinkage. The forward scatter in FACS analysis was thus used to estimate the cell size. As shown in

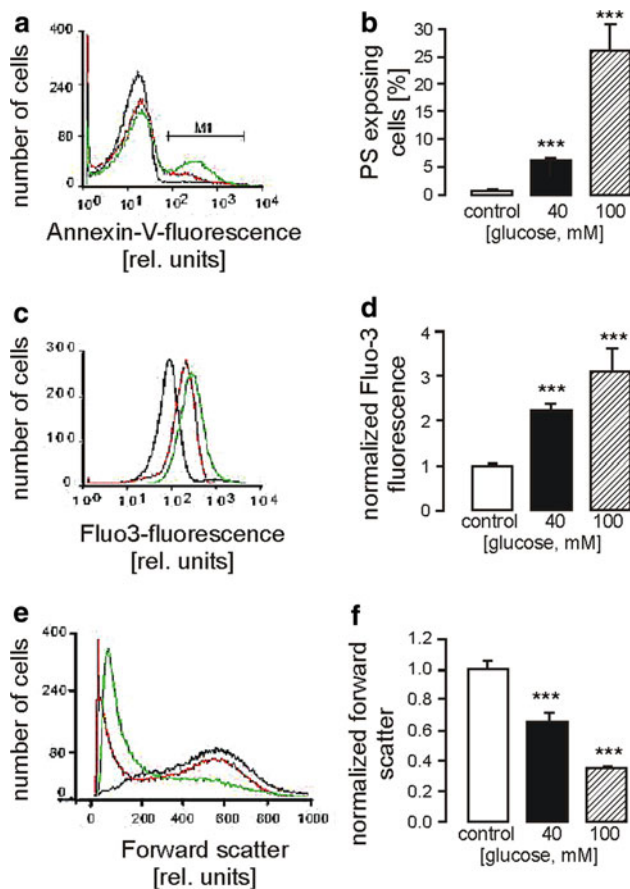


Fig. 2 Effect of high glucose treatment on phosphatidylserine exposure, forward scatter and cytosolic free Ca^{2+} concentration. **(a)** Histogram of annexin V binding in a representative experiment of human erythrocytes exposed 48 h to isotonic Ringer solution (*black line*), to Ringer solution with 40 mM glucose added (*gray*) and to Ringer solution with 100 mM glucose added (*light gray*). **(b)** Arithmetic means \pm SEM of the percentage of annexin V-binding erythrocytes after a 48-h treatment with Ringer solution in the absence (*white bar*, $n = 17$) and presence of 40 mM glucose (*black bar*, $n = 12$) or 100 mM glucose (*hatched bar*, $n = 5$). *** Significant difference from control, $P < 0.001$, ANOVA. **(c)** Histogram of Fluo-3 fluorescence in a representative experiment of human erythrocytes exposed 48 h to isotonic Ringer solution (*black line*), to Ringer solution with 40 mM glucose added (*red line*) and to Ringer solution with 100 mM glucose added (*green line*). **(d)** Arithmetic means \pm SEM of normalized Fluo3 fluorescence of erythrocytes after a 48-h treatment with Ringer solution in the absence (*white bar*, $n = 19$) and presence of 40 mM glucose (*black bar*, $n = 12$) or 100 mM glucose (*hatched bar*, $n = 7$). *** Significant difference from control, $P < 0.001$, ANOVA. **(e)** Histogram of forward scatter (FCS) in a representative experiment of erythrocytes exposed 48 h to isotonic Ringer solution (*black line*), to Ringer solution with 40 mM glucose added (*red line*), and to Ringer solution with 100 mM glucose added (*green line*). **(f)** Arithmetic means \pm SEM of normalized FCS of erythrocytes after a 48-h treatment with Ringer solution in the absence (*white bar*, $n = 19$) and presence of 40 mM glucose (*black bar*, $n = 12$) or 100 mM glucose (*hatched bar*, $n = 7$). *** Significant difference from control, $P < 0.001$, ANOVA

Fig. 2e, f, the exposure to high glucose concentrations resulted in a substantial and statistically significant decrease of forward scatter pointing to cell shrinkage.

Again, the effect was significantly more pronounced after exposure to 100 mM glucose than after exposure to 40 mM glucose (Fig. 2f).

The Ca^{2+} -induced cell shrinkage is thought to result from activation of Gardos K^+ channels (Bookchin et al. 1987; Brugnara et al. 1993). Cell-attached patch clamp experiments with K^+ -containing pipette solution confirmed activation of K^+ channels similar to Gardos channels after glucose treatment. Channel activity was virtually lacking in untreated cells (Fig. 3a, c) but was observed after glucose treatment (Fig. 3b, c). The current–voltage relationship (I/V) curve with 150 mM KCl pipette solution revealed inward rectification of the channels (Fig. 3g).

To better define the Ca^{2+} entry pathway stimulated by glycation, we recorded patch clamp whole-cell currents from control erythrocytes (5 mM glucose) and experimentally glycosylated cells (40 mM or 100 mM glucose for 48 h). When combining Na–gluconate pipette and NaCl Ringer bath solution (Fig. 4a, upper tracings, and Fig. 4b, open triangles), whole-cell currents tended to increase with increasing glycation. Replacing bath Na^+ by the larger and less permeable cation NMDG $^+$ decreased the inward currents in all three groups and shifted the reversal potentials of the current–voltage relationships from ~ 10 mV in NaCl Ringer solution (Fig. 4b, open triangles) to about -50 mV in NMDG-Cl bath solution (Fig. 4b, closed triangles). This indicates that the principal whole-cell current fraction in control and experimentally glycosylated cells was cation selective. Accordingly, the conductance (calculated for the inward currents by linear regression) declined after substitution of bath Na^+ with NMDG $^+$. As shown in Fig. 4c, the conductance decline was significantly larger in glycosylated cells than in control cells ($P \leq 0.05$, ANOVA). Taken together, these experiments reveal a glycation-stimulated activation of cation channels in human erythrocytes.

Next, we characterized the amiloride sensitivity and the Ca^{2+} permeability of these channels. Earlier studies revealed that millimolar (mM) concentrations of amiloride are required to inhibit the channels (Duranton et al. 2002; Huber et al. 2001; Lang et al. 2003c). Addition of amiloride (2 mM) to the NaCl Ringer bath (Na–gluconate in the pipette) decreased outward and inward currents of all three groups (Fig. 5a, upper and middle tracings). Upon wash-out, currents reappeared only partially. In Fig. 5b, the amiloride-sensitive current fractions of all three groups are plotted against the voltage. The amiloride-sensitive current fractions reversed near 0 mV voltage and increased with experimental glycation. The latter is also shown in Fig. 5c by the amiloride-sensitive conductances calculated for the inward currents of control (5 mM glucose) and experimentally glycosylated cells (40 and 100 mM glucose, respectively). To assess the Ca^{2+} permeability of the glycation-activated currents, NaCl Ringer solution in the bath was

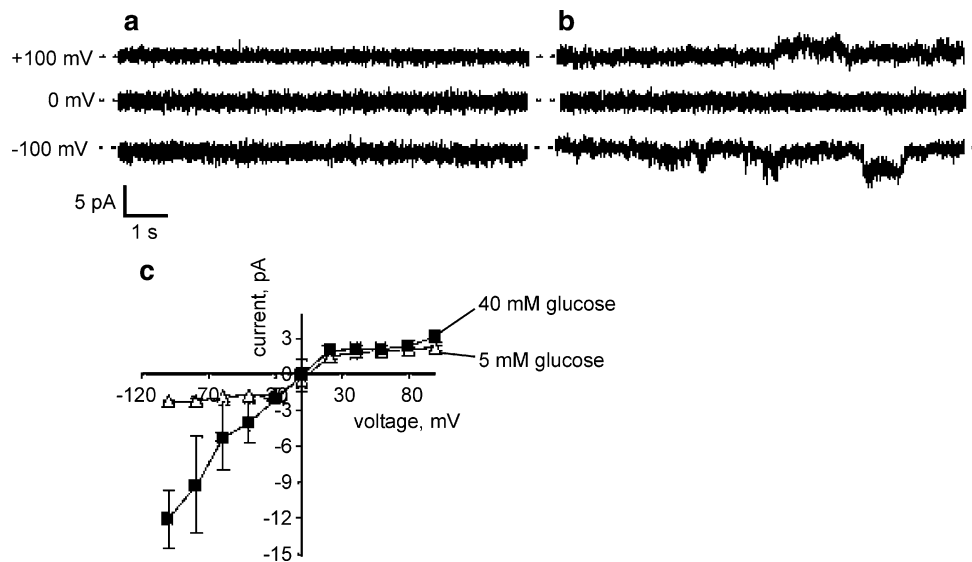


Fig. 3 Effect of high glucose treatment on Gardos channel activity. (a, b) Current traces (at -100 , 0 , and $+100$ mV) recorded in cell-attached mode using KCl pipette and NaCl Ringer bath solution in control (5 mM glucose) cells (A) and experimentally glycated erythrocytes (40 mM glucose for 48 h, B). (c) Mean (\pm SE, $n = 3$)

I/V relationships of the macroscopic currents recorded in cell-attached mode using KCl pipette and NaCl Ringer solution in control (5 mM glucose, *open triangles*) cells (a) and experimentally glycated erythrocytes (40 mM glucose for 48 h, *closed squares*, b)

replaced by CaCl_2 (100 mM). As shown in Fig. 5d, high Ca^{2+} concentrations blocked the current in all three groups.

Because high Ca^{2+} concentrations reportedly may inhibit cation channels (Lemonnier et al. 2006; Shi et al. 2004), we recorded whole-cell currents of control (5 mM glucose) and glycated (40 mM glucose) erythrocytes with NMDG-Cl in the bath (Cs-aspartate in the pipette, Fig. 6a, c closed squares) and added 10 mM of CaCl_2 extracellularly (Fig. 6a, c, open triangles). As a result, the inward currents increased in both groups, and the reversal potentials changed toward more positive values (Fig. 6a, c). Figure 6b, d shows the 10 mM CaCl_2 -dependent current fractions. They approximated 0 pA at high positive voltages, indicating that they were carried by Ca^{2+} influx into the cells ($E_{\text{Ca}} > +200$ mV). Importantly, this Ca^{2+} current was significantly higher in glycated (40 mM glucose) than in control cells (5 mM glucose), as shown by the CaCl_2 -dependent conductances (as calculated for the entire voltage range by linear regression) in Fig. 6d. The glycation-dependent and Ca^{2+} -carried currents were observed at negative voltages, suggesting that they were not gated by positive voltages.

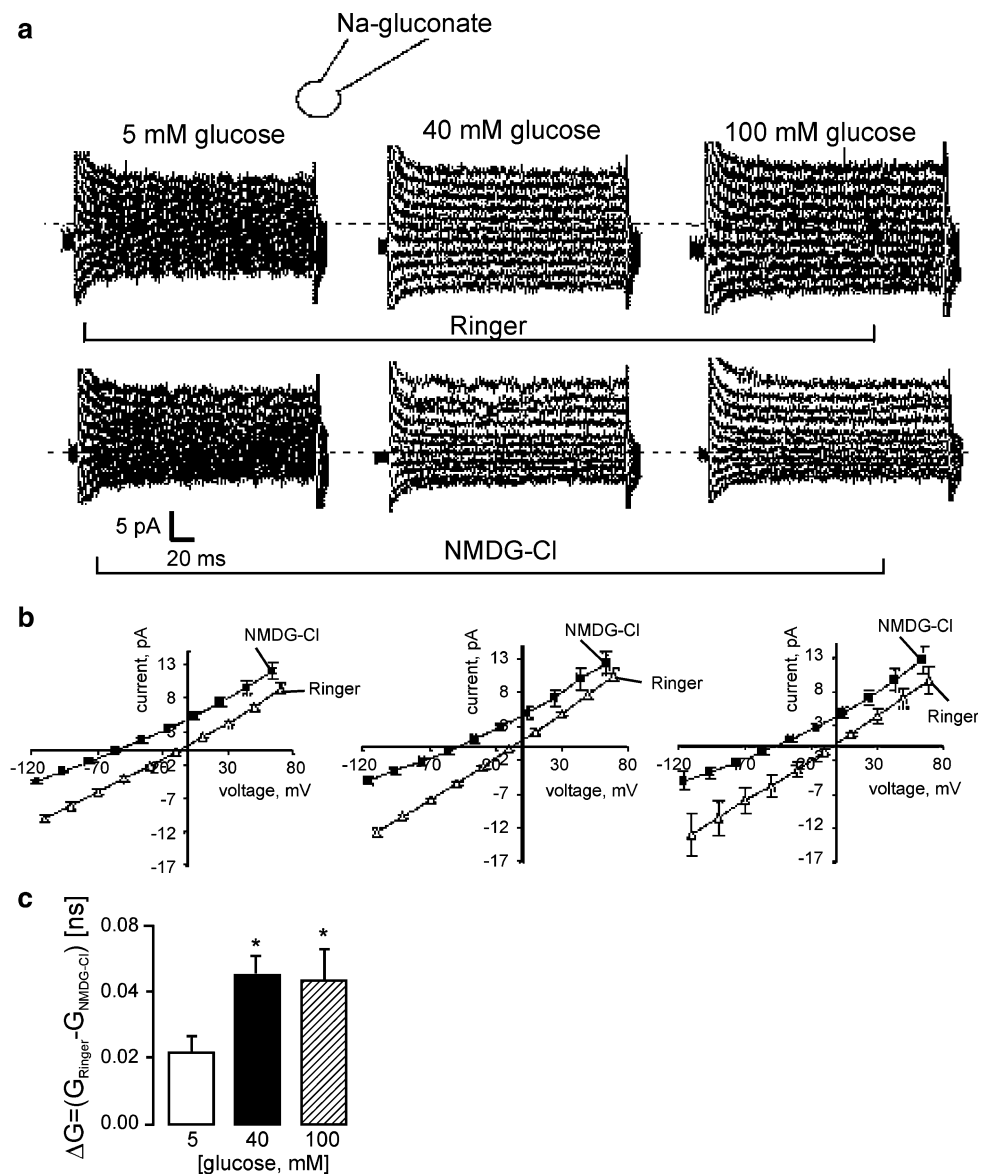
Finally, we tested whether the glycation-stimulated current fraction is dependent on extracellular Cl^- by replacing NaCl Ringer solution in the bath by Na-gluconate (Na-gluconate in the pipette). As shown in Fig. 7a, removal of extracellular Cl^- led to a small current increase in all three groups. These Cl^- -dependent cation currents did not differ significantly between the groups, as

additionally clarified by the calculated conductances in Fig. 7c. In summary, experimental glycation activated amiloride-sensitive extracellular Cl^- -independent cation channels in human erythrocytes.

The increase in cation conductance and in $[\text{Ca}^{2+}]_i$ strongly suggested that the observed cell membrane scrambling and cell shrinkage after exposure to high glucose concentrations were due to Ca^{2+} entry. To estimate the contribution of Ca^{2+} entry to the observed cell membrane scrambling and cell shrinkage, additional experiments were performed in the nominal absence of extracellular Ca^{2+} (i.e., after removal of free Ca^{2+} by addition of Ca^{2+} chelator EGTA). As shown in Fig. 8, the removal of extracellular Ca^{2+} indeed abrogated the increase of Fluo3 fluorescence (Fig. 8c, d) and the decrease of forward scatter (Fig. 8e, f). Annexin V binding still tended to increase (Fig. 8a, b)—an effect, however, not reaching statistical significance ($P = 0.139$ and $P = 0.379$ for 40 mM and 100 mM glucose, respectively, $n = 4$).

Western blot depicting advanced glycated end products revealed an increase in the total amount of glycated membrane proteins after incubation with high (40 and 100 mM) glucose (Fig. 9). The proteins of band 1 (~ 200 kDa), band 3 (~ 100 kDa), band 4.2 (~ 70 kDa), band 5 (~ 50 kDa), and low-molecular-weight proteins (~ 20 kDa) were found to be modified by in vitro glycation in high-glucose-containing Ringer solutions. The effect was concentration dependent, and the density of glycated proteins was particularly

Fig. 4 Experimental glycation activates cation channels in human erythrocytes. **(a)** Whole-cell current tracings of erythrocytes incubated for 48 h in control medium (5 mM glucose) or in media with elevated glucose concentration (40 or 100 mM). Currents were recorded with Na-gluconate pipette and NaCl Ringer bath solution (*upper tracings*) and upon replacement of the bath Ringer solution by NMDG-Cl (*lower tracings*). **(b)** Mean (\pm SE, $n = 3-8$) I/V relationships recorded as in A with NaCl Ringer solution (*open triangles*) or with NMDG-Cl (*closed squares*) from control erythrocytes (5 mM glucose, *left*), and cells glycated with 40 mM (*middle*) or 100 mM glucose (*right*). **(c)** Mean (\pm SE, $n = 3-8$) conductance decline (as calculated from the data in **(b)**) for the inward currents by linear regression) of control (5 mM glucose, *open bar*) and cells glycated with 40 mM (*closed bar*) or 100 mM glucose (*hatched bar*). * $P \leq 0.05$, ANOVA



enhanced in 100 mM glucose-treated cells. Western immunoblots further revealed the existence of TRPC3/6/7 proteins in human erythrocytes (Fig. 9c). The TRPC3/6/7 proteins were found to be affected by high-glucose treatment (Fig. 9b). There was a significant increase in glycation of TRPC3/6/7 channel proteins after a 2-day treatment with 100 mM glucose (Fig. 9d). Glycation of L-type channels ($\alpha 1C$ proteins) similarly tended to increase after high-glucose treatment—an effect, however, not reaching statistical significance (Fig. 10).

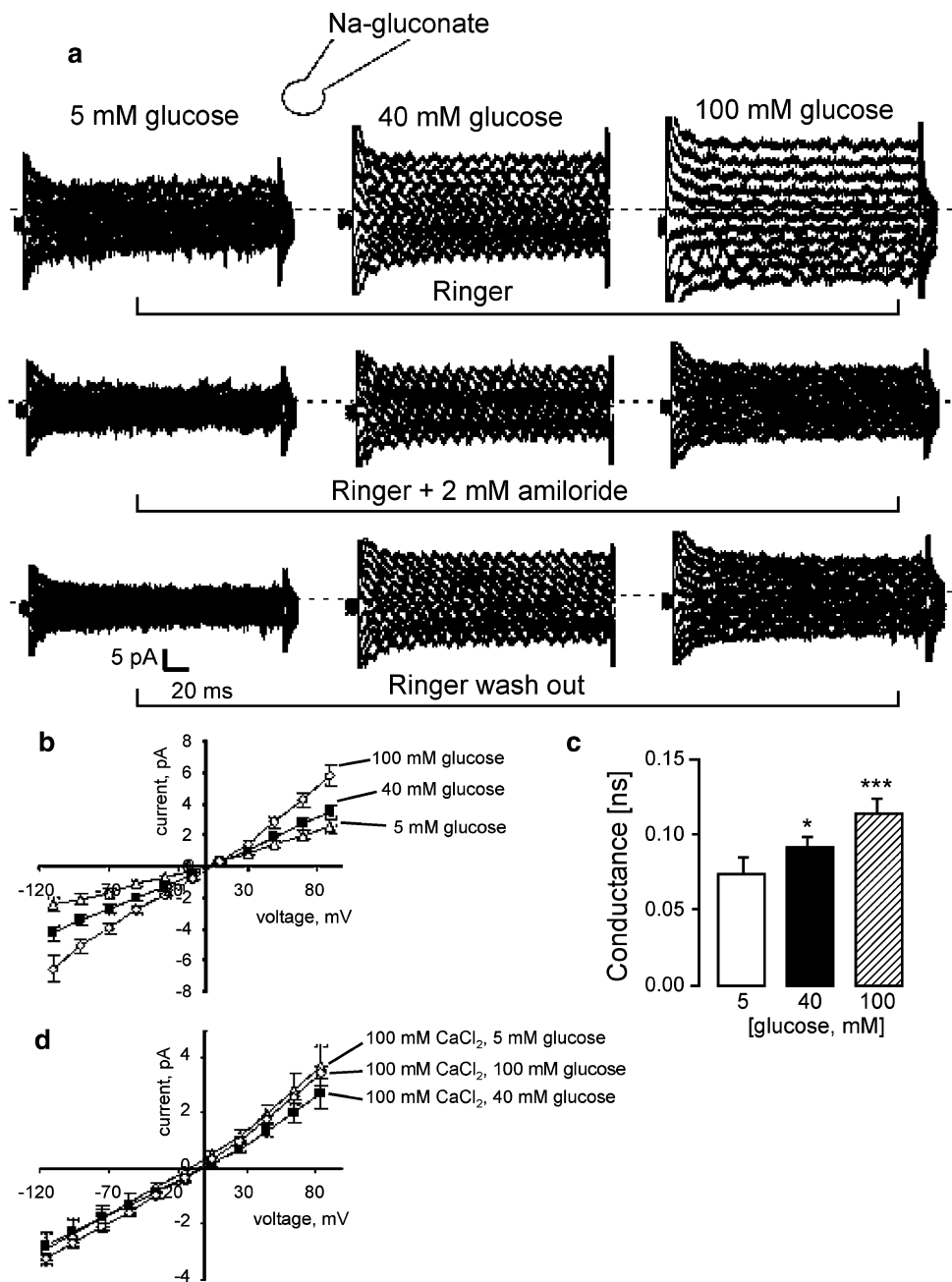
Discussion

The present study confirms that exposure to high glucose concentrations leads to stimulation of hemoglobin as well

as membrane protein glycation. In addition, our data reveal that short-term high glucose treatment triggers the activity of Ca^{2+} -permeable amiloride-sensitive cation channels, an increase in $[\text{Ca}^{2+}]_i$, cell membrane scrambling, and cell shrinkage. Most importantly, the present observations show that increase of $[\text{Ca}^{2+}]_i$, cell membrane scrambling, and cell shrinkage after glycation are prevented by removal of Ca^{2+} from the extracellular fluid.

To our knowledge, the role of cation channels in artificially aged (glycated) human erythrocytes has not been shown before. The observed slight but statistically significant increase of the cation current (Fig. 4) presumably contributed to the increase of $[\text{Ca}^{2+}]_i$. According to electrophysiology, human erythrocytes express both voltage-gated (Baunbaek and Bennekou 2008) and voltage-independent (Huber et al. 2001) cation channels. The

Fig. 5 The glycation-activated cation channels are amiloride-sensitive and blocked by high extracellular Ca^{2+} concentrations. **(a)** Current tracings (Na-gluconate pipette and NaCl Ringer bath solution) recorded in control (5 mM glucose, *left*) and glycated (40 mM, *middle*, and 100 mM glucose, *right*) erythrocytes before (*upper tracings*), during (*middle tracings*), and after (washout, *lower tracings*) bath application of amiloride (2 mM). **(b)** Mean (\pm SE, $n = 5-6$) I/V relationships of the amiloride-sensitive current fractions of control cells (5 mM glucose, *open triangle*), 40 mM glucose- (*closed squares*) and 100 mM glucose-glycated (*open diamond*) erythrocytes. **(c)** Mean (\pm SE, $n = 5-6$) amiloride-sensitive conductance (as calculated from the data in **(b)**) for the inward currents by linear regression) of control (5 mM glucose, *open bar*) and cells glycated with 40 mM (*closed bar*) or 100 mM glucose (*hatched bar*). * ** $P \leq 0.05$ and $P \leq 0.001$, respectively, ANOVA. **(d)** Mean (\pm SE, $n = 3-4$) I/V relationships of control (5 mM glucose, *open triangle*), 40 mM glucose- (*closed squares*) and 100 mM glucose-glycated (*open diamond*) erythrocytes recorded with Na-gluconate in the pipette and 100 mM CaCl_2 in the bath solution



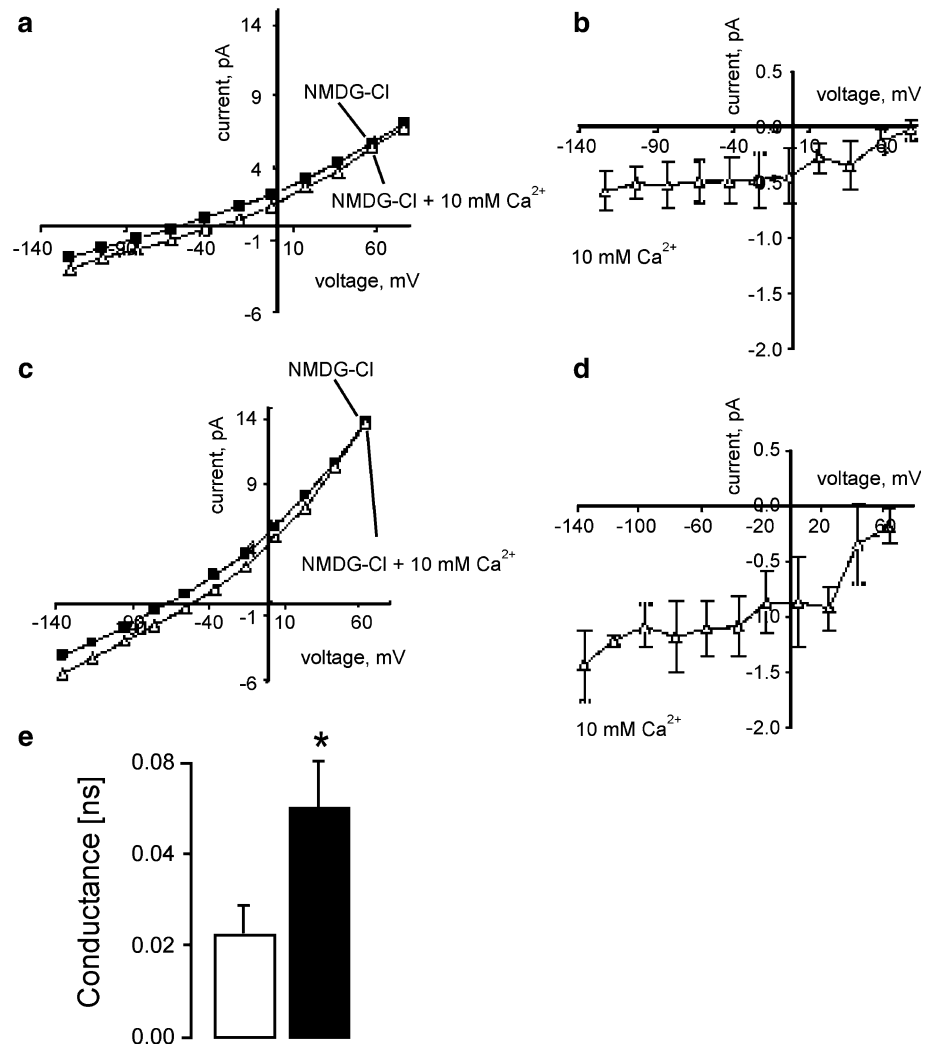
voltage-independent cation channels were shown to be partially related to TRPC6 channels (Foller et al. 2008). Moreover, the presence of subtypes of voltage-dependent Ca^{2+} channels has recently been demonstrated by Western blot analysis in membranes of young and senescent erythrocytes (Romero et al. 2006).

The nonselective voltage-dependent cation channels were found to be active at high positive potentials (more than +40 mV) (Bennekou 1993; Kaestner et al. 2000) and thus probably do not account for the increase in cation conductance observed in the glucose-treated cells. The channels activated resemble rather the nonselective voltage-

independent cation channels in human erythrocytes activated after osmotic shock, oxidation, and removal of extracellular Cl^- (Lang et al. 2008). In the present study, the Cl^- removal-induced cation current activation was not affected by experimental glycation, suggesting that glycation does not interfere with the signaling triggered by Cl^- removal.

In theory, the channels and eryptosis could have been activated by an increase of osmolarity due to addition of 40 and 100 mM glucose to Ringer solution. However, the osmolarity required to stimulate the channels and eryptosis is much higher than the osmolarity utilized here (Lang

Fig. 6 Glycation-stimulates voltage-independent Ca^{2+} currents. **(a, c)** Mean ($n = 3-4$) I/V relationships of control (5 mM glucose, **a**) and glycated (40 mM glucose, **c**) human erythrocytes recorded in whole-cell mode with Cs-aspartate pipette and 160 mM NMDG-Cl bath solution before (*closed squares*) and after addition of 10 mM CaCl_2 (*open triangles*) to the bath solution. **(b, d)** Mean I/V relationships (\pm SE, $n = 3-4$) of the current fractions in control (**b**) and glycated erythrocytes (**d**) that increased upon bath addition of 10 mM Ca^{2+} . **(e)** Mean (\pm SE, $n = 3-4$) conductance increase of control (5 mM glucose, *open bar*) and glycated (40 mM glucose, *closed bar*) erythrocytes after bath addition of 10 mM CaCl_2 . Conductance increases were calculated from the current fractions in **(b, d)** by linear regression; * $P \leq 0.05$, *t*-test



et al. 2003b). Moreover, the channels have previously been shown to be activated by addition of sucrose (Lang et al. 2003b), which does not enter and thus shrinks the cells, whereas glucose readily enters erythrocytes via the glucose transporter GLUT1 (Montel-Hagen et al. 2009). Glucose redistribution depends on its concentration in the bath medium and on the time and temperature of incubation (Greene 1965). After addition of extracellular glucose at a concentration of 144 mM, intracellular glucose concentration increases within 5 min to ~ 65 mM and within 120 min to 119 mM (Greene 1965). At lower bath concentrations, glucose was shown to almost equally distribute between cells and bath solution (Greene 1965). Accordingly, acute addition of 100 mM glucose did not trigger a cation current (data not shown).

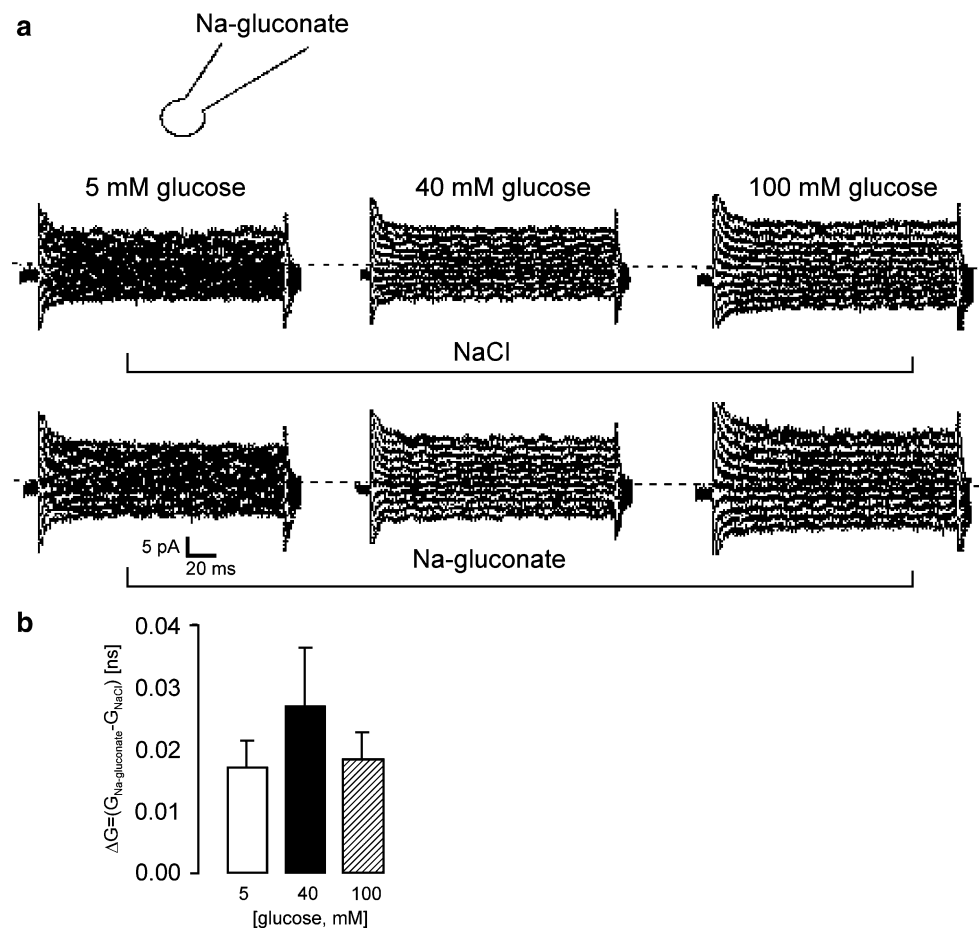
Besides its effect on glycation, glucose may trigger the formation of oxygen-reactive species (Jain and Lim 2001), which in turn is known to activate the cation channels (Duranton et al. 2002). However, oxidative stress is rapidly effective—and again, acute exposure of erythrocytes to

100 mM glucose did not appreciably alter cation conductance.

High glucose concentration might alter $[\text{Ca}^{2+}]_i$ by directly glycating ion channels. The present study indeed observed glycation of one or more members of the TRPC3/6/7 subfamily of canonical TRP channels and possibly a L-type Ca^{2+} channel subunit by Western blot analysis. However, the linear I/V relationship of the glycation-activated cation conductance neither resembled those of the TRP channels (Dietrich et al. 2003; Shi et al. 2004) nor showed any voltage-dependent gating typical for L type Ca^{2+} channels.

It is noteworthy that the effect of glycation on the cation current is small and that additional mechanisms may also have contributed to the net Ca^{2+} entry. Erythrocyte aging is paralleled by a decrease of the plasma membrane Ca^{2+} pump activity. Similarly, glycation could increase $[\text{Ca}^{2+}]_i$, followed by an increase in phosphatidylserine exposure, in part by impairing Ca^{2+} extrusion by the ATPase plasma membrane Ca^{2+} pump (Bilgin and Tükel 1996; Gonzalez

Fig. 7 Experimental glycation does not modify the activation of cation currents by removal of extracellular Cl^- (a) Current tracings of control (5 mM glucose, *left*) and glycated (40 mM, *middle*, and 100 mM glucose, *right*) erythrocytes recorded with Na-gluconate pipette and NaCl Ringer bath solution (*upper tracings*) and after removal of extracellular Cl^- by superfusion of Na-gluconate (*lower tracings*). (b) Mean (\pm SE, $n = 7$ –10) of Cl^- -dependent conductance, calculated as a difference of the conductances in Na-gluconate and NaCl bath media



Flecha et al. 1999; Lew et al. 2007). The activity of the pump may not be directly affected by glycation (Raftos et al. 2001), but its function may be compromised indirectly.

An increase of $[\text{Ca}^{2+}]_i$ leads to activation of Ca^{2+} -sensitive K^+ channels (Bookchin et al. 1987; Brugnara et al. 1993) with subsequent hyperpolarization, which is expected to drive Cl^- exit in parallel to the cellular loss of K^+ (Schneider et al. 2007). Our on-cell patch clamp experiments confirmed activation of the Gardos channels after high glucose treatment (Fig. 3). The activation of the channels was presumably due to increased cytosolic Ca^{2+} concentration. In Ca^{2+} loaded cells, erythrocyte senescence was paralleled by decrease of Gardos channel activity (Tiffert et al. 2007). The main changes in the ionic content of aging erythrocytes are loss of intracellular K^+ and the gradual accumulation of Na^+ and Ca^{2+} (Lew et al. 2007).

The increase of $[\text{Ca}^{2+}]_i$ is further known to trigger cell membrane scrambling, leading to phosphatidylserine exposure at the cell surface (Lang et al. 2003b). Cell membrane scrambling is indeed stimulated by enhanced glycation, as previously described (Quan et al. 2006), and additionally confirmed by the present study.

$[\text{HbA}_{1c}]$ is not only increased after aging (Gram-Hanssen et al. 1990; Lew et al. 2007), but is also highly increased in patients with diabetes (Cukiernik et al. 2004; Ditzel et al. 1979; Hileeto et al. 2002; Mortensen and Brahm 1985; Wu et al. 2008). Accordingly, diabetes leads to enhanced cell membrane scrambling (Labrousche et al. 1996). As phosphatidylserine-exposing erythrocytes are recognized by macrophages, they are rapidly removed from the circulating blood (Kuypers and de Jong 2004). A subpopulation of red blood cells exposes phosphatidylserine in humans with diabetes, and the size of this subpopulation of cells is related to blood glucose levels (Manodori and Kuypers 2002). Accordingly, the turnover of erythrocytes is accelerated in mice with diabetes (Manodori and Kuypers 2002).

In conclusion, our experiments demonstrate that in vitro glycation of human erythrocytes results in a significant increase in HbA_{1c} , phosphatidylserine exposure, and $[\text{Ca}^{2+}]_i$, accompanied by a decrease in cell volume—all phenomena paralleling the events of progressive erythrocyte aging. The effects require Ca^{2+} entry from the extracellular space and are at least partially due to activation of Ca^{2+} -permeable cation channels.

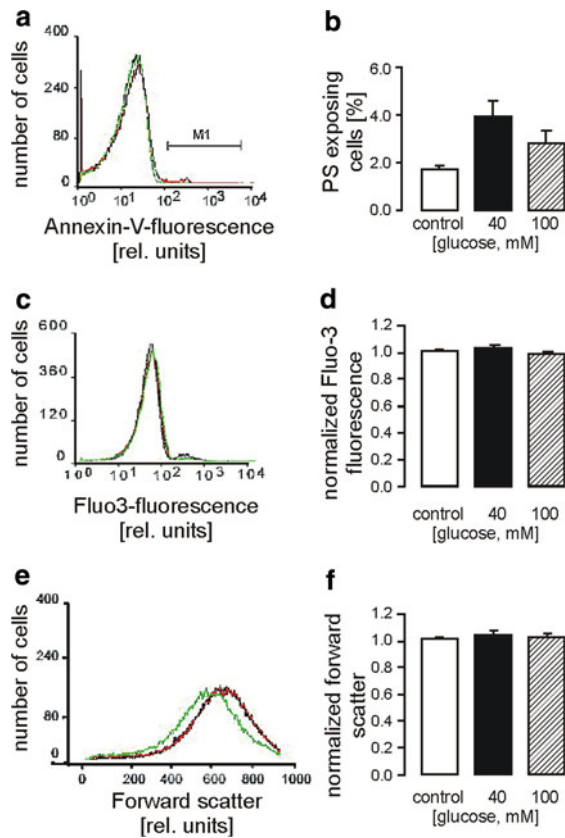


Fig. 8 Effect of high glucose treatment on phosphatidylserine exposure, cytosolic free Ca^{2+} and forward scatter in low Ca^{2+} -containing media. (a) Histogram of annexin V binding in a representative experiment of erythrocytes exposed 48 h to isotonic Ringer solution containing 5 mM EGTA (black line), to Ringer solution containing 5 mM EGTA with 40 mM glucose added (gray) and to Ringer solution containing 5 mM EGTA with 100 mM glucose added (light gray). (b) Arithmetic means \pm SEM of the percentage of annexin V-binding erythrocytes exposed 48 h to isotonic Ringer solution containing 5 mM EGTA (white bar, $n = 4$), to Ringer solution containing 5 mM EGTA with 40 mM glucose added (black bar, $n = 4$) and to Ringer solution containing 5 mM EGTA with 100 mM glucose added (hatched bar, $n = 4$). (c) Histogram of Fluo-3 fluorescence in a representative experiment of erythrocytes exposed 48 h to isotonic Ringer solution containing 5 mM EGTA (black line), to Ringer solution containing 5 mM EGTA with 40 mM glucose added (red line) and to Ringer solution containing 5 mM EGTA with 100 mM glucose added (green line). (d) Arithmetic means \pm SEM of normalized Fluo3 fluorescence of erythrocytes exposed 48 h to isotonic Ringer solution containing 5 mM EGTA (white bar, $n = 4$), to Ringer solution containing 5 mM EGTA with 40 mM glucose added (black bar, $n = 4$) and to Ringer solution containing 5 mM EGTA with 100 mM glucose added (hatched bar, $n = 4$). (e) Histogram of forward scatter in a representative experiment of erythrocytes exposed 48 h to isotonic Ringer solution containing 5 mM EGTA (black line), to Ringer solution containing 5 mM EGTA with 40 mM glucose added (red line) and to Ringer solution containing 5 mM EGTA with 100 mM glucose added (green line). (f) Arithmetic means \pm SEM of normalized forward scatter of erythrocytes exposed 48 h to isotonic Ringer solution containing 5 mM EGTA (white bar, $n = 4$), to Ringer solution containing 5 mM EGTA with 40 mM glucose added (black bar, $n = 4$) and to Ringer solution containing 5 mM EGTA with 100 mM glucose added (hatched bar, $n = 4$)

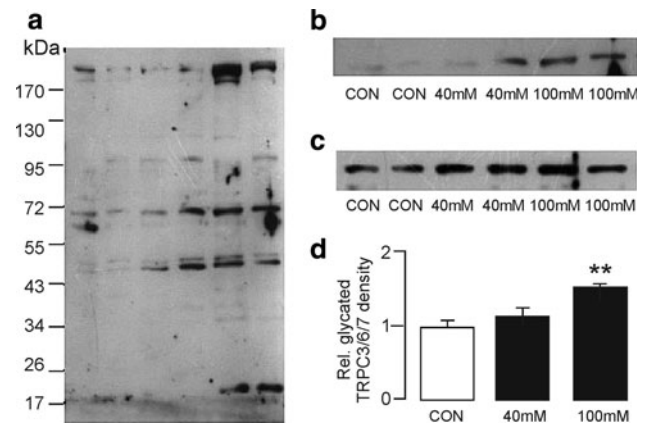


Fig. 9 Western blot of glycated erythrocyte membrane proteins and immunoblots of native and glycated TRPC3/6/7 proteins. (a) Original Western blot of glycated erythrocyte membrane proteins: control samples (CON); erythrocytes incubated in 40 mM glucose (40 mM) and 100 mM glucose (100 mM) containing Ringer solutions, respectively. (b) Original Western blot of glycated TRPC3/6/7 proteins in human erythrocytes upon 2 days' incubation in 40 mM and 100 mM glucose. (c) Original Western blot of TRPC3/6/7 proteins in the erythrocyte membrane. (d) Arithmetic mean \pm SEM ($n = 4$) of glycosylated to nonglycosylated TRPC3/6/7 proteins densities. ** Significant difference from control, $P < 0.001$, ANOVA

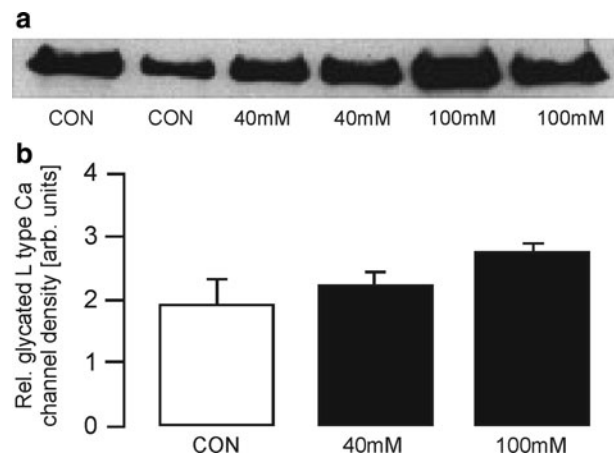


Fig. 10 Western immunoblot of glycated L-type Ca^{2+} ($\alpha 1\text{C}$ peptide) channels. Original Western blot of glycated L-type (human $\alpha 1\text{C}$ peptide) proteins in human erythrocytes upon 2 days' incubation in 40 mM and 100 mM glucose

Acknowledgments The authors gratefully acknowledge the support by the Deutsche Akademischer Austauschdienst (DAAD). They declare that they have no conflict of interest.

References

- Arai K, Maguchi S, Fujii S et al (1987) Glycation and inactivation of human Cu-Zn-superoxide dismutase. Identification of the in vitro glycosylated sites. *J Biol Chem* 262:16969–16972
- Avogaro A, de Kreutzenberg SV, Fadini GP (2010) Insulin signaling and life span. *Pflugers Arch* 459:301–314

- Barry PH, Lynch JW (1991) Liquid junction potentials and small cell effects in patch-clamp analysis. *J Membr Biol* 121:101–117
- Baunbaek M, Bennekou P (2008) Evidence for a random entry of Ca^{2+} into human red cells. *Bioelectrochemistry* 73:145–150
- Bennekou P (1993) The voltage-gated non-selective cation channel from human red cells is sensitive to acetylcholine. *Biochim Biophys Acta* 1147:165–167
- Bilgin R, Tukul SS (1996) Effects of glucose on the activity of erythrocyte membrane Ca^{2+} ATPase in subjects with normal and impaired glucose tolerance. *Biochem Mol Biol Int* 39:547–552
- Bookchin RM, Ortiz OE, Lew VL (1987) Activation of calcium-dependent potassium channels in deoxygenated sickled red cells. *Prog Clin Biol Res* 240:193–200
- Bookchin RM, Etzion Z, Lew VL et al (2009) Preserved function of the plasma membrane calcium pump of red blood cells from diabetic subjects with high levels of glycated haemoglobin. *Cell Calcium* 45:260–263
- Booth AA, Khalifah RG, Todd P et al (1997) In vitro kinetic studies of formation of antigenic advanced glycation end products (AGEs). Novel inhibition of post-Amadori glycation pathways. *J Biol Chem* 272:5430–5437
- Brugnara C, de Franceschi L, Alper SL (1993) Inhibition of Ca^{2+} -dependent K^{+} transport and cell dehydration in sickle erythrocytes by clotrimazole and other imidazole derivatives. *J Clin Invest* 92:520–526
- Bunn HF, Higgins PJ (1981) Reaction of monosaccharides with proteins: possible evolutionary significance. *Science* 213:222–224
- Chen G, Frohlich O, Yang Y et al (2006) Loss of N-linked glycosylation reduces urea transporter UT-A1 response to vasopressin. *J Biol Chem* 281:27436–27442
- Chu X, Tong Q, Cheung JY et al (2004) Interaction of TRPC2 and TRPC6 in erythropoietin modulation of calcium influx. *J Biol Chem* 279:10514–10522
- Cukiernik M, Hileeto D, Downey D et al (2004) The role of the sodium hydrogen exchanger-1 in mediating diabetes-induced changes in the retina. *Diabetes Metab Res Rev* 20:61–71
- Dietrich A, Schnitzler M, Emmel J et al (2003) N-linked protein glycosylation is a major determinant for basal TRPC3 and TRPC6 channel activity. *J Biol Chem* 278:47842–47852
- Ditzel J, Nielsen NV, Kjaergaard JJ (1979) Hemoglobin A1c and red cell oxygen release capacity in relation to early retinal changes in newly discovered overt and chemical diabetics. *Metabolism* 28:440–447
- Duranton C, Huber SM, Lang F (2002) Oxidation induces a Cl^{-} -dependent cation conductance in human red blood cells. *J Physiol* 539:847–855
- Fluckiger R, Winterhalter KH (1976) In vitro synthesis of hemoglobin A1c. *FEBS Lett* 71:356–360
- Foller M, Kasinathan RS, Koka S et al (2008) TRPC6 contributes to the Ca^{2+} leak of human erythrocytes. *Cell Physiol Biochem* 21:183–192
- Gonzalez Flecha FL, Castello PR, Gagliardino JJ et al (1999) Molecular characterization of the glycated plasma membrane calcium pump. *J Membr Biol* 171:25–34
- Gram-Hansen P, Mourits-Andersen HT, Eriksen JE et al (1990) Glycosylated haemoglobin (HbA1c) as an index of the age of the erythrocyte population in non-diabetic patients. *Eur J Haematol* 44:201–203
- Greene NM (1965) Glucose permeability of human erythrocytes and effects of inhalation anesthetics oxygen and carbon dioxide. *Yale J Biol Med* 37:319–330
- Hileeto D, Cukiernik M, Mukherjee S et al (2002) Contributions of endothelin-1 and sodium hydrogen exchanger-1 in the diabetic myocardium. *Diabetes Metab Res Rev* 18:386–394
- Huber SM, Gamper N, Lang F (2001) Chloride conductance and volume-regulatory nonselective cation conductance in human red blood cell ghosts. *Pflügers Arch* 441:551–558
- Jain SK, Lim G (2001) Pyridoxine and pyridoxamine inhibits superoxide radicals and prevents lipid peroxidation, protein glycosylation, and $(\text{Na}^{+} \text{K}^{+})$ -ATPase activity reduction in high glucose-treated human erythrocytes. *Free Radic Biol Med* 30:232–237
- Kaestner L, Christophersen P, Bernhardt I et al (2000) The non-selective voltage-activated cation channel in the human red blood cell membrane: reconciliation between two conflicting reports and further characterisation. *Bioelectrochemistry* 52:117–125
- Kuypers FA, de Jong K (2004) The role of phosphatidylserine in recognition and removal of erythrocytes. *Cell Mol Biol (Noisy-le-grand)* 50:147–158
- Labrousse S, Freyburger G, Gin H et al (1996) Changes in phospholipid composition of blood cell membranes (erythrocyte, platelet, and polymorphonuclear) in different types of diabetes—clinical and biological correlations. *Metabolism* 45:57–71
- Lang F, Lang KS, Wieder T et al (2003a) Cation channels, cell volume and the death of an erythrocyte. *Pflügers Arch* 447:121–125
- Lang KS, Duranton C, Poehlmann H et al (2003b) Cation channels trigger apoptotic death of erythrocytes. *Cell Death Differ* 10:249–256
- Lang KS, Myssina S, Tanneur V et al (2003c) Inhibition of erythrocyte cation channels and apoptosis by ethylisopropylamiloride. *Naunyn Schmiedebergs Arch Pharmacol* 367:391–396
- Lang F, Gulbins E, Lerche H et al (2008) Eryptosis, a window to systemic disease. *Cell Physiol Biochem* 22:373–380
- Lemonnier L, Trebak M, Lievreumont JP et al (2006) Protection of TRPC7 cation channels from calcium inhibition by closely associated SERCA pumps. *FASEB J* 20:503–505
- Lew VL, Daw N, Etzion Z et al (2007) Effects of age-dependent membrane transport changes on the homeostasis of senescent human red blood cells. *Blood* 110:1334–1342
- Manodori AB, Kuypers FA (2002) Altered red cell turnover in diabetic mice. *J Lab Clin Med* 140:161–165
- Montel-Hagen A, Sitbon M, Taylor N (2009) Erythroid glucose transporters. *Curr Opin Hematol* 16:165–172
- Mortensen HB, Brahm J (1985) Glucose transport in erythrocytes of diabetic and healthy children as related to hemoglobin A1c. *Clin Chem* 31:1387–1389
- Quan GB, Liu MX, Ren SP et al (2006) Changes of phosphatidylserine distribution in human red blood cells during the process of loading sugars. *Cryobiology* 53:107–118
- Raftos JE, Edgley A, Bookchin RM et al (2001) Normal Ca^{2+} extrusion by the Ca^{2+} pump of intact red blood cells exposed to high glucose concentrations. *Am J Physiol Cell Physiol* 280:C1449–C1454
- Romero PJ, Romero EA, Mateu D et al (2006) Voltage-dependent calcium channels in young and old human red cells. *Cell Biochem Biophys* 46:265–276
- Schneider J, Nicolay JP, Foller M et al (2007) Suicidal erythrocyte death following cellular K^{+} loss. *Cell Physiol Biochem* 20:35–44
- Shapiro HM (2003) Practical flow cytometry, 4th edn. Wiley, p 736
- Shi J, Mori E, Mori Y et al (2004) Multiple regulation by calcium of murine homologues of transient receptor potential proteins TRPC6 and TRPC7 expressed in HEK293 cells. *J Physiol* 561:415–432
- Tiffert T, Bookchin RM, Lew VL (2003) Calcium homeostasis in normal and abnormal human red cells. In: Bernhardt I, Ellory JC (eds) Red cell membrane transport in health and disease. Springer Verlag, New York, pp 373–405

- Tiffert T, Daw N, Etzion Z et al (2007) Age decline in the activity of the Ca^{2+} -sensitive K^{+} channel of human red blood cells. *J Gen Physiol* 129:429–436
- Turker EM, Young JD (1982) A methodological approach. In: Red cell membranes. Academic Press, London, 31–41
- Vannier B, Zhu X, Brown D et al (1998) The membrane topology of human transient receptor potential 3 as inferred from glycosylation-scanning mutagenesis and epitope immunocytochemistry. *J Biol Chem* 273:8675–8679
- Vlassara H, Fuh H, Makita Z et al (1992) Exogenous advanced glycosylation end products induce complex vascular dysfunction in normal animals: a model for diabetic and aging complications. *Proc Natl Acad Sci USA* 89:12043–12047
- Wu S, Song T, Zhou S et al (2008) Involvement of $\text{Na}^{+}/\text{H}^{+}$ exchanger 1 in advanced glycation end products-induced proliferation of vascular smooth muscle cell. *Biochem Biophys Res Commun* 375:384–389